

COMMUNICATION

Chemoenzymatic Dynamic Kinetic Resolution of Primary Benzylic Amines using Pd(0)-CalB CLEA as a Biohybrid Catalyst

Karl P. J. Gustafson,^[†,a,b] Tamás Görbe,^[†,a] Gonzalo de Gonzalo,^[a] Ning Yuan,^[b,c] Cynthia Schreiber,^[a] Andrey Shchukarev,^[d] Cheuk-Wai Tai,^[b] Ingmar Persson,^[c] Xiaodong Zou,^[b] and Jan-E. Bäckvall*^[a]

[†]These author contributed equally to this work

Abstract: Herein, we report on the use a biohybrid catalyst consisting of palladium nanoparticles immobilized on cross-linked enzyme aggregates of lipase B of *Candida antarctica* (CalB CLEA) for the dynamic kinetic resolution (DKR) of benzylic amines. A set of amines were demonstrated to undergo an efficient DKR and the recyclability of the catalysts was studied. Extensive efforts to further elucidate the structure of the catalyst are presented.

Recent developments in materials science and nanotechnology have greatly accelerated the field of heterogeneous catalysis. Today, a large number of catalysts, ranging from organometallic complexes to enzymes, can be efficiently immobilized onto heterogeneous supports.^[1] Most heterogeneous catalysts used in different organic transformations rely on the concept of having a support onto which the catalyst can be immobilized.^[2] The co-immobilization of different catalysts can in certain cases improve the efficiency of the reaction even further.^[3] To make use of these co-immobilized species, the reaction design requires the orchestration of coupling reactions which exploits the reactivity of all the immobilized catalytically active species.^[4] Previously our group reported on the co-immobilization of Pd nanoparticles^[5] and the enzyme *Candida antarctica* lipase B (CalB) into the cavities of a siliceous mesocellular foam (MCF) and demonstrated the use of this nanohybrid catalyst in dynamic kinetic resolution (DKR) of amines.^[6] An intrinsic drawback with this immobilization is that the amount of the catalytically active species is still quite low compared to the total mass of the solid material. The performance of heterogeneous biocomposite catalysts has emerged during the past few years.^[7] Both the Zare^[8] and the

Palomo^[9] groups have studied a promising design of bifunctional catalysts, where enzyme solutions are converted to heterogeneous catalysts. Inspired by their research we have applied a more rationally designed system, where an aggregate of the CalB enzyme is formed by cross-linking with glutaraldehyde, which creates a well-established spherical heterogeneous material. The application of such cross-linked enzyme aggregates (CLEAs) in process chemistry has been well illustrated in many examples.^[10] Moreover, as the CLEA itself constitutes the heterogeneous phase, it can also be considered to be biodegradable and to exhibit rather low toxicity. The use of CLEA as a support for metal nanoparticles to generate bifunctional biohybrid catalysts may therefore be a possible alternative to improve the applicability and scalability of metal-enzyme composites.

Recently, our group reported the synthesis of a Pd(0)-CalB CLEA catalyst. This catalyst was successfully used in a cascade reaction, where 4-pentynoic acid was cycloisomerized by Pd to an *exo*-cyclic vinyl lactone which was used *in situ* as acyl donor in a CalB-catalyzed kinetic resolution of *sec*-alcohols.^[11] Unfortunately, the Pd(0) catalyst was not able to racemize the *sec*-alcohols as required for a DKR and therefore the cascade enzyme acylation of the alcohol was limited to a kinetic resolution. During this work, we became interested in using this biohybrid catalyst for DKR of amines,^[12] since the Pd(0) of the composite is expected to racemize amines. A few years after the first report by Reetz, the group of Bäckvall reported the use of Shvo's catalysts as the first homogeneous catalyst employed in the DKR of amines. To date this Ru protocol is still the most versatile protocol, applicable to both benzylic and aliphatic amines.^[14,15] At the same time as Bäckvall's publication, the group of De Vos and Jacobs independently described the use of palladium nanoparticles immobilized on alkaline salts as racemization catalyst in the chemoenzymatic DKR of benzylic amines.^[16] In subsequent work several other similar heterogeneous systems were reported for DKR of amines^[6,17,18,19,20,21,22,23] including a nanohybrid catalyst.^[6] One intrinsic drawback with all these heterogeneous protocols is that the catalysts employed consist of an excess inert material as support. With this in mind we wanted to explore the use of the previously described Pd(0)-CalB CLEA bifunctional biohybrid catalyst for DKR of amines.

The Pd(0)-CalB CLEA biohybrid catalyst was previously characterized using different microscopic techniques. To complement the results from the previous studies other techniques such as X-ray Photoelectron Spectroscopy (XPS), X-ray Absorption Spectroscopy (XAS) and annular dark-field

[a] Dr. K. P. J. Gustafson, Dr. T. Görbe, Dr. G. de Gonzalo-Calvo, C. Schreiber, Prof. Dr. J.-E. Bäckvall
Department of Organic Chemistry, Arrhenius Laboratory
Stockholm University
SE-106 91, Stockholm (Sweden)
E-mail: jeb@organ.su.se

[b] Dr. C.-W. Tai, N. Yuan, Prof. Dr. X. Zou
Department of Materials and Environmental Chemistry
Stockholm University
SE-106 91, Stockholm (Sweden)

[c] Prof. Dr. I. Persson
Department of Molecular Sciences
Swedish University of Agricultural Sciences
SE-106 91, Uppsala, Sweden

[d] Dr. A. Shchukarev
Department of Chemistry
Umeå University
SE-750 07, Umeå, Sweden

COMMUNICATION

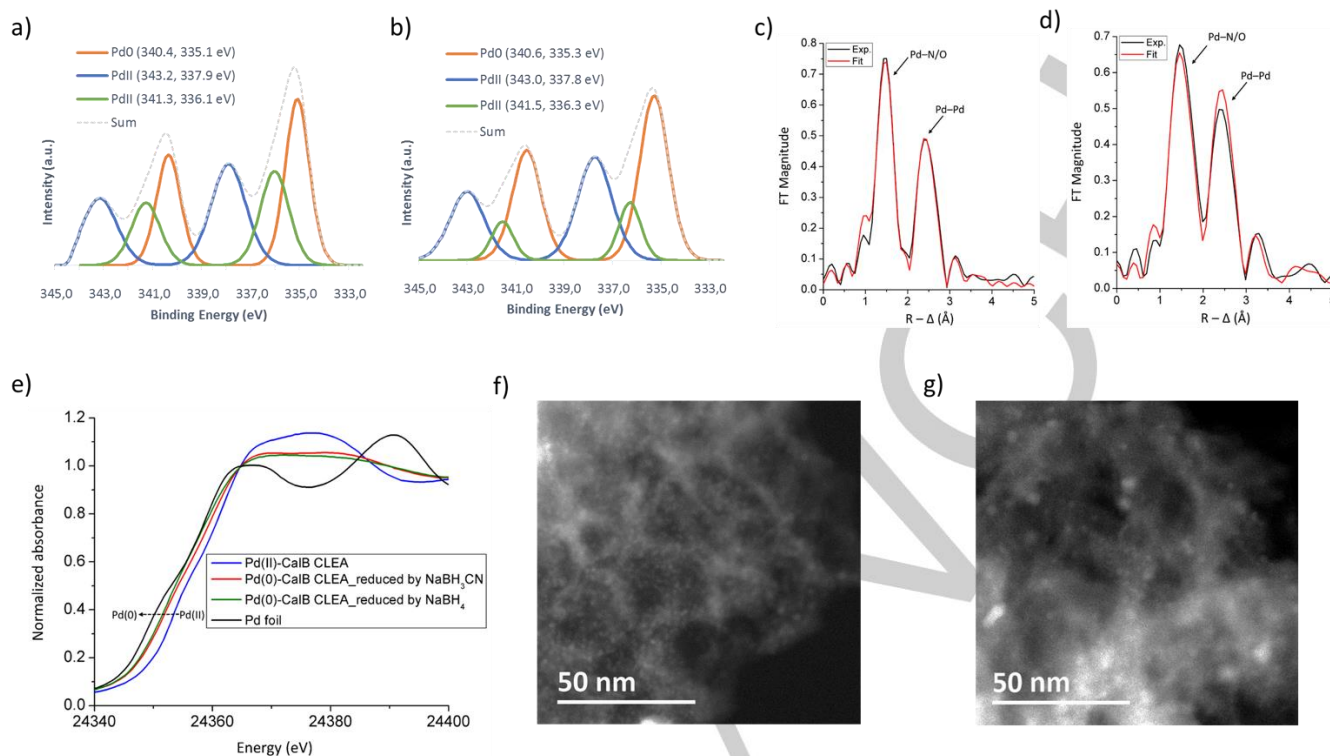


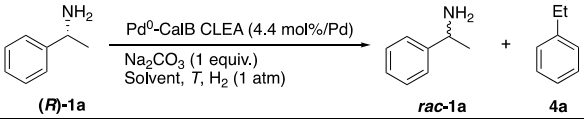
Figure 1. XPS spectrum of Pd $3d^{5/2}$ of catalyst reduced with a) NaBH_3CN and b) NaBH_4 . Fourier transformed k^2 -weighted EXAFS spectra of catalysts reduced with c) NaBH_3CN and d) NaBH_4 . The spectra are not phase corrected. e) Normalized Pd K-edge XANES spectra of the pre-catalyst, the reduced catalyst and Pd foil reference. HAADF-STEM images of catalyst reduced with f) NaBH_3CN and g) NaBH_4 .

scanning transmission electron microscopy (HAADF-STEM) studies were carried out on the Pd(0)-CalB CLEA catalyst (Figure 1). Also, the effect of two different reducing agents (NaBH_4 vs. NaBH_3CN) for the generation of the palladium nanoparticles were studied. When comparing the Pd $3d^{5/2}$ signals in the XPS spectrum of the two catalysts from the two reductions it was clear that the catalyst reduced by NaBH_4 contained more reduced Pd (Pd(0)) relative to the catalyst reduced by NaBH_3CN (Figure 1a and b, Pd(0) signal at 335.1 eV relative to overall: 1:1.5 (NaBH_3CN) and 1:1 (NaBH_4)). The two catalysts showed an intriguing composition of different Pd(II)-species, the species were present in different ratios in the two catalysts (signal at 336.1 eV relative to the one at 338.0 eV). The catalysts were further compared by extended X-ray absorption fine structure (EXAFS), and their Fourier transformed spectra are presented in Figure 1c-d. Similarities were observed in both the mononuclear region (Pd-N/O, ~ 1.5 Å without phase correction) and the region corresponding to the Pd nanoparticle (Pd-Pd, ~ 2.4 Å without phase correction) (Figure 1c-d). Interestingly, the relative magnitude of the Pd-Pd peak in Figure 1d appears slightly higher than that in Figure 1c, which corresponds to a minor difference in the average coordination number of Pd-Pd derived from refinement of the spectra (Table S5). This can be attributed to a larger fraction of Pd nanoparticles in the catalyst reduced by NaBH_4 than that reduced by NaBH_3CN . The X-ray absorption near edge structure (XANES) spectra (Figure 1e) show that the edge positions of Pd in the reduced catalysts are between the positions of Pd(II) pre-catalyst and metallic palladium. This means that the Pd(II) and Pd(0) species coexist in the catalysts, which agrees well with the observations from XPS and EXAFS. With a closer look, the edge position of Pd in the catalyst reduced by NaBH_4

lies at a slightly lower energy than the catalyst reduced by NaBH_3CN , and their edge shape profile features are not identical. These details support our conclusion that there are more Pd nanoparticles in the catalyst reduced by NaBH_4 , and hint as well that the Pd(II) species in these two catalysts could be different. However, the HAADF-STEM of the two catalysts did not show enough significant differences that allowed to draw any conclusions concerning the relative amount of Pd(0) and Pd(II) (Figure 1f and g).

After previously demonstrating that the Pd-CLEA biocomposite is capable of catalyzing kinetic resolutions, the focus now was on optimizing the racemization of amines. Initial attempts to racemize α -methyl benzylamine (*R*)-**1a**, using the previously prepared catalyst (where NaBH_3CN was employed as reducing agent for generating Pd-nanoparticles) yielded poor racemization. A change of the reducing agent from the mild NaBH_3CN to the more strongly reducing NaBH_4 , gave a catalyst with an enhanced rate of racemization. Initial attempts to use the latter catalyst (with 4.4 mol% Pd) in toluene at 90 °C under 1 atm of hydrogen gas led to racemization, where enantiomerically pure amines (*R*)-**1a** afforded the semi-racemized amine in 31% ee after 6 h. However, the by-product ethylbenzene **4a** was also formed in substantial amounts (Table 1, entry 1).^[24] By the use of other solvents such as 1,4-dioxane and THF, the side-product **4a** was formed in smaller amounts, however, at the same time the rate of racemization went down (entries 2-3). Attempts to reduce the side product formation further by lowering the temperature (entries 4-5), changing other ethereal solvents, or lowering the concentration were unsuccessful (See supporting information, Table S1).

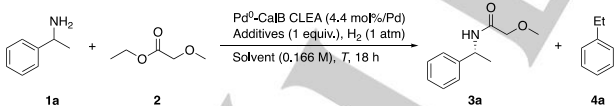
COMMUNICATION

Table 1. Optimization table for the racemization of (*R*)-1a.^[a]


Entry ^[a]	Solvent	T [°C]	t [h]	ee [%] ^[b]	4a [%] ^[c]
1	Toluene	90	6	31	29
2	1,4-Dioxane	90	6	62	9
3	THF	90	6	58	3
4	THF	60	6	94	<1
5	1,4-Dioxane	60	6	96	<1

[a] Reaction conditions: **1a** (0.25 mmol, 0.166 M), Pd(0)-CalB CLEA (22 mg, 4.4 mol% Pd) under 1 atm of hydrogen gas at 90 °C. [b] ¹HGC-FID with chiral column. [c] Determined using NMR yield with 1,3,5-trimethoxybenzene as internal standard.

After establishing the limits of the Pd-catalyzed racemization, the focus was directed to find the optimal reaction conditions for DKR of **1a**. From previous successful studies in our group and by others,^[23,25] 2 equiv. of ethyl methoxyacetate was employed as acyl donor at 90 °C using Na₂CO₃ as drying agent/acid scavenger in toluene at a concentration of 0.166 M (Table 2, entry 1). Gratifyingly, amide **3a** was obtained in 81% yield with an ee of 95%. Changing the solvent to 1,4-dioxane marginally improved the yield and ee of amide **3a**, however, the main improvement was seen in that the conversion to the by-product ethyl benzene **4a** was reduced from 19% to 5% (entry 2). Changing the solvent to THF improved the ee and further reduced the amount of ethyl benzene **4a**, however, the yield was slightly reduced to 65% (entry 3). Other ethereal solvents were screened, but they did not improve the results (see Supporting Information, Table S2). When the base was changed to other organic or inorganic bases, no further improvement of the reaction was observed (entries 5-7).

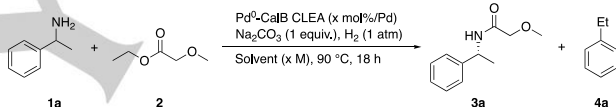
Table 2. Optimization of the DKR of 1a with regards to additives, temperature and solvent.^[a]


Entry	Solvent	Base	T [°C]	3a [%] ^[b]	ee [%] ^[c]	4a [%] ^[b]
1	Toluene	Na ₂ CO ₃	90	81	95	19
2	1,4-Dioxane	Na ₂ CO ₃	90	82	96	5
3	THF	Na ₂ CO ₃	90	65	99	<1
4	THF	Na ₂ CO ₃	60	60	99	<1

5	THF	K ₂ CO ₃	60	45	99	<1
6	THF	NaOAc	60	53	99	<1
7	THF	TEA	60	66	91	<1

[a] Reaction conditions: **1a** (0.25 mmol, 0.166 M), Pd(0)-CalB CLEA (22 mg, 4.4 mol% Pd) under 1 atm of hydrogen gas at 90 °C. [b] Determined using NMR yield with 1,3,5-trimethoxybenzene as internal standard. [c] GC-FID with chiral column.

In an attempt to increase the yield of the DKR, different concentrations were tried, and with an increase of the concentration to 0.25 M the yields were improved in 1,4-dioxane and THF, to 87% and 82% yield, respectively (Table 3, entries 1-2). The ee was slightly higher in THF than in 1,4-dioxane. In toluene on the other hand, the results were not affected or got slightly worse (entry 3) on increasing the concentration. An additional increase of the concentration in THF and 1,4-dioxane improved the yield, however, the ee became lower and no overall improvement was obtained (entries 4-5). When increasing or decreasing the catalyst loading, no improvement of the reaction was observed (entries 6-7).

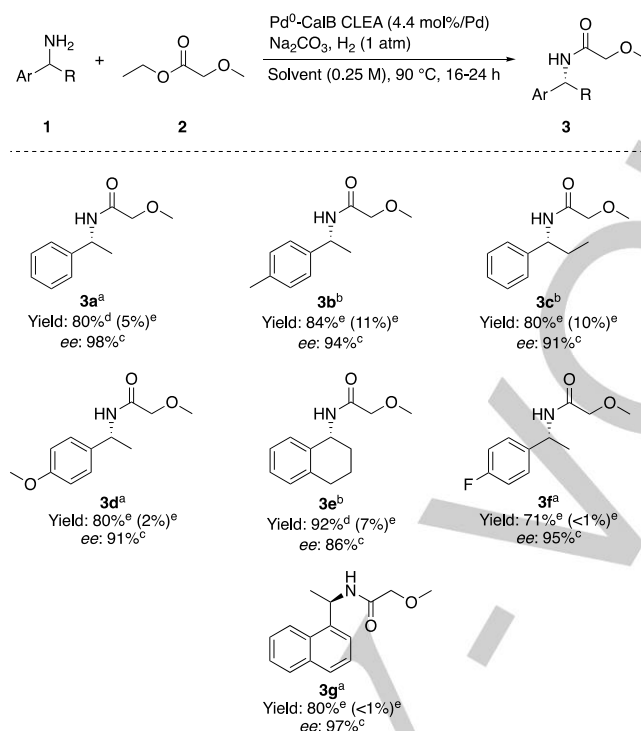
Table 3. Optimization of concentration and catalyst loading in the DKR of 1a.^[a]


Entry	Solvent	1a [M]	Pd [mol%]	3a [%] ^[b]	ee [%] ^[c]	4a [%] ^[b]
1	1,4-Dioxane	0.25	4.4	87	94	5
2	THF	0.25	4.4	82	98	5
3	Toluene	0.25	4.4	77	93	18
4	THF	0.5	4.4	83	95	6
5	1,4-Dioxane	0.5	4.4	90	92	10
6	1,4-Dioxane	0.25	2.2	82	93	3
7	1,4-Dioxane	0.25	8.8	83	93	17

[a] Reaction conditions: **1a** (0.25 mmol), Pd(0)-CalB CLEA (22 mg, 4.4 mol% Pd) under 1 atm of hydrogen gas at 90 °C. [b] Determined using NMR yield with 1,3,5-trimethoxybenzene as internal standard. [c] GC-FID with chiral column.

After the optimized reaction conditions had been established for the DKR of the amines (using 4.4 mol% of catalyst) in either 1,4-dioxane or THF (0.25 M) at 90 °C and Na₂CO₃ as base under 1 atm of hydrogen, differently substituted benzylic amines were studied in the reaction (Scheme 1). All the chiral amides **2a-g**

COMMUNICATION



Scheme 1. Substrate scope of the DKR of amines catalyzed by Pd(0)-CalB CLEA. [a] Reaction conditions: **1a** (0.25 mmol), **2** (0.5 mmol), Pd(0)-CalB CLEA (22 mg, 4.4 mol% Pd), dry Na₂CO₃ (28 mg, 0.26 mmol) in THF (0.25 M) under 1 atm of hydrogen gas at 90 °C. [b] Reaction was performed in 1,4-dioxane (0.25 M). [c] Product ee was determined by using chiral column on GC or HPLC. [d] Isolated yield. [e] NMR-yield of product **3** or the equivalent debenzylated structure.

were obtained in good yields and in good to high ee. In general, it was established that the use of 1,4-dioxane led to higher conversions but resulted in an increased amount of side product **4a-g** (around 10%), while the use of THF afforded higher selectivities and lower amounts of side product compared to 1,4-dioxane.

To demonstrate the recyclability of the biohybrid catalyst Pd(0)-CalB CLEA, the DKR of (*rac*)-1-phenylethylamine **1a** in 1,4-dioxane and toluene at 90 °C was performed over four and five cycles, as shown in Figure 2a and 2b. After each cycle, the reaction mixture was separated by centrifugation, in order to recover the solid catalyst. The recovered solid catalyst was successively washed with 2 mL of phosphate buffer (0.1 M, pH 7.2), 2 mL of acetone and 2 mL of diethyl ether. As shown in Figure 2a, the catalyst activity and enantioselectivity decreased when 1,4-dioxane was used as solvent. Already in the second the

ee dropped from 95% to 86%. After the first two cycles the yield and ee was reduced even further. Recycling in toluene (Figure 1b), was more successful and after the first three cycles the yield only dropped slightly from 78% to 72% and the ee changed from 95% to 92%. In the following cycles the yield and ee were reduced further.

Because of the significant deactivation of the catalyst used in 1,4-dioxane, the HAADF-STEM, XAS and XPS were carried out on the recovered catalyst to gain information concerning the deactivation. The leaching was first tested but in neither 1,4-dioxane nor toluene any significant leaching could be detected (Pd <0.5 ppm), showing that deactivation was not due to leaching. The XPS spectrum of Pd in the reused catalyst did not change significantly and was comparable to the spectrum of the starting catalyst.

COMMUNICATION

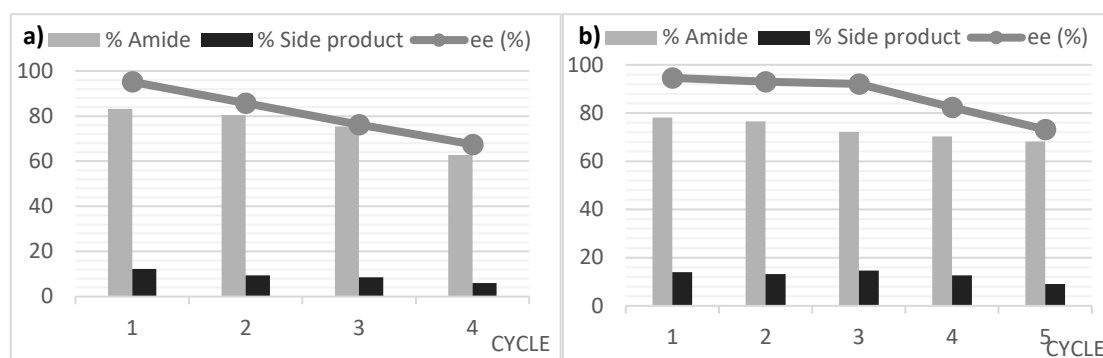


Figure 2. Recycling of Pd(0)-CalB CLEA in the DKR of 1-phenylethylamine **1a** at 90 °C: a) in 1,4-dioxane and b) in toluene.

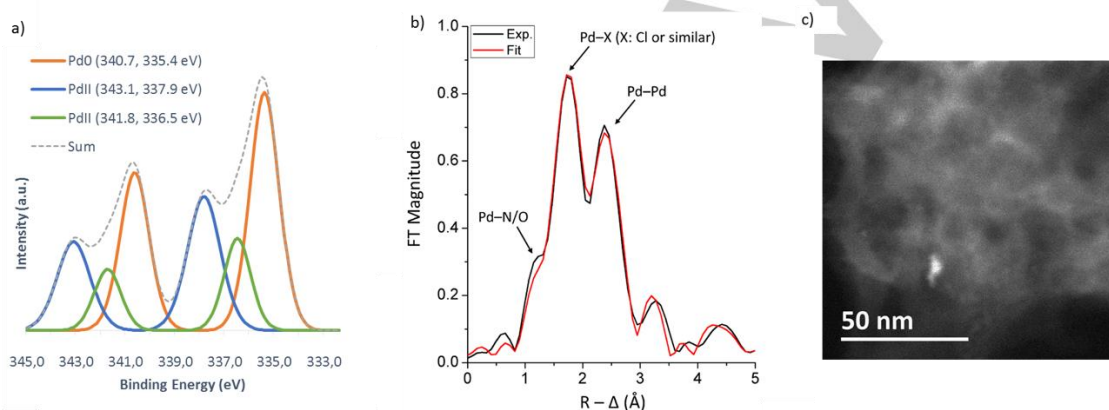


Figure 3. a) XPS spectrum of Pd 3d_{5/2} of the reused catalyst in 1,4-dioxane. b) Fourier transformed k₃-weighted EXAFS spectrum of the reused catalyst in 1,4-dioxane. The spectrum is not phase corrected. c) HAADF-STEM of the reused catalyst in 1,4-dioxane.

When examining the EXAFS spectrum of the reused catalyst (Figure 3b) the same peaks as in fresh catalyst (Pd-N/O and Pd-Pd) could be observed. Unlike in the spectrum of the unused catalyst a second peak had appeared at 1.9 Å (not phase corrected), suggesting that a new bond previously not present had been formed. The bond distances according to the best fit was determined to be 2.29 Å (Table S6). This distance is in the range of a Pd-Cl or Pd-S (XPS spectrum of S 2p did not indicate a significant change in the sulphur, which suggest another element than S (Figure S4). This new bond can arise from contamination of chloride ions in the reagents and solvents. In an attempt to get a visual support of the deactivation, the catalyst was examined by electron microscopy (HAADF-STEM). It is obvious from the HAADF-STEM images that Pd had agglomerated and in certain regions of the material Pd had been washed out (Figure 3c).

Herein we have reported the continued structure elucidation of the Pd(0)-CalB CLEA using different techniques such as TEM, XPS and XAS. Gratifyingly, the Pd biocomposite was successfully implemented in the DKR of primary amines using a set of benzylic amines and the results compare very well with previously developed DKRs of amines. The strength of this approach is that a new type of hybrid catalyst is used in the DKR as an artificial

metalloenzyme.²⁶ This type of cross-linked enzymes with immobilized nanometal particles is promising and should open up new opportunities in the area of dynamic kinetic resolution. Interesting structural changes were observed in the catalyst recycled in 1,4-dioxane, and the appearance of a Pd-Cl or Pd-S bond or similar bond was observed in the Fourier transformed EXAFS, that most likely arise from impurities after destabilization of the Pd nanoparticles in 1,4-dioxane. Continued efforts in the research group will be focused on improving the synthesis of CLEA biohybrids, and to explore new reactivities of the reported catalyst, as well as to make new biocomposite materials for catalysis.

Experimental Section

General procedure for the dynamic kinetic resolution (DKR) of **1.** Into a flame-dried Schlenk flask were added dry Na₂CO₃ (0.28 mmol, 30 mg), Pd(0)-CalB CLEA (22 mg) and 1,3,5-trimethoxybenzene (16.8 mg, 0.1 mmol). The reaction vessel was evacuated and refilled with hydrogen gas three times. Then, dry solvent (1.0 mL), the corresponding racemic amine

COMMUNICATION

1a-g (0.25 mmol), and ethyl methoxyacetate (0.5 mmol, 59 μL) were added and the system was evacuated and followed by refilling with hydrogen gas. The mixture was heated to the indicated temperatures and stirred for the times established. After reaching completion, reactions were filtered with ethyl acetate through Celite® plug. The NMR yield of the final amides (*R*)-**3a-g** and the amount of the ethyl benzene **4a** obtained as by-product were determined by $^1\text{H-NMR}$ using 1,3,5-trimethoxybenzene as internal standard or isolated using silica gel chromatography (gradient 0-40% EtOAc in pentane) while the optical purity of the amides (*R*)-**3a-f** was determined by GC. Enantiomeric excess of compound (*R*)-**3g** was determined by HPLC.

Acknowledgements

Financial support from The Swedish Research Council (2016-03897, 2015-04099), the Berzelii Center EXSELENT, and the Knut and Alice Wallenberg Foundation (KAW 2016.0072) is gratefully acknowledged. Gonzalo de Gonzalo thanks MINECO (Ramón y Cajal Program) for personal funding.

Keywords: heterogeneous catalysis • key cross-linked enzyme aggregates • dynamic kinetic resolution • amide • biohybrid catalyst

- [1] a) M. Peixoto de Almeida, S. A. C. Carabineiro, *ChemCatChem* **2012**, *4*, 18–29; b) Q. Yang, D. Han, H. Yang, C. Li, *Chem. Asian J.* **2008**, *3*, 1214–1229; c) A. Zsigmond, F. Notheisz, *Curr. Org. Chem.* **2006**, *10*, 1655–1680. For organo catalysts see: d) R. Munirathinam, J. Huskens, W. Verboom, *Adv. Synth. Catal.* **2015**, *357*, 1093–1123; e) C. Rodriguez-Escrich, M. Pericas, *Eur. J. Org. Chem.* **2015**, 1173–1188; f) T. Tsubogo, T. Ishiwata, S. Kobayashi, *Angew. Chem. Int. Ed.* **2013**, *52*, 6590–6604. For nanoparticles see: g) S. Peiris, J. McMurtrie, H. Y. Zhu, *Catal. Sci. Technol.* **2016**, *6*, 320–338; h) L. L. Chng, N. Erathodiyil, J. Y. Ying, *Acc. Chem. Res.* **2013**, *46*, 1825–1837; i) K. An, G. A. Somorjai, *ChemCatChem* **2012**, *4*, 1512–1524; j) D. Astruc, F. Lu, J. R. Aranzaes, *Angew. Chem. Int. Ed.* **2005**, *44*, 7852–7872. For biocatalysts see: k) Y. Zhang, J. Ge, Z. Liu, *ACS Catal.* **2015**, *5*, 4503–4513; l) J. M. Bolivar, I. Eisl, B. Nidetzky, *Catal. Today* **2015**, *259*, 66–80; m) P. Adlercreutz, *Chem. Soc. Rev.* **2013**, *42*, 6406–6436; n) R. DiCosimo, J. McAuliffe, A. J. Poulouse, G. Bohlmann, *Chem. Soc. Rev.* **2013**, *4*, 6437–6474.
- [2] a) D. S. Su in *Nanomaterials in Catalysis*, 1st ed. (Eds.: P. Serp, K. Phillipot), Wiley-VCH, Weinheim, **2013**, pp. 331–374; b) L. F. Malbena, S. Sinha Ray, S. D. Mhlanga, N. J. Coville, *Appl. Nanosci.* **2011**, *1*, 67–77; c) M. B. Gawande, P. S. Branco, R. S. Varma, *Chem. Soc. Rev.* **2013**, *42*, 3371–3393; d) V. Hulea, E. Dumitriu in *Nanomaterials in Catalysis*, 1st ed. (Eds.: P. Serp, K. Phillipot), Wiley-VCH, Weinheim, **2013**, pp 375–413; e) M. Flytzani-Stephanopoulos, B. C. Gates, *Annu. Rev. Chem. Biomol. Eng.* **2012**, *3*, 545–574; f) R. Luque, A. M. Balu, M. Campelo, M. D. Gracia, E. Losada, A. Pineda, A. A. Romero, J. C. Serrano-Ruiz, *Catalysis* **2012**, *24*, 253–280; g) D. Astruc, *Inorg. Chem.* **2007**, *46*, 1884–1894.
- [3] a) R. Srivastava, B. Sarmah, B. Satpati, *RSC Adv.* **2015**, *5*, 25998–26006; b) Y. Horiuchi, D. Do Van, Y. Yonezawa, M. Saito, M. Dohshi, T. H. Kim, M. Matsuoka, *RSC Adv.* **2015**, *5*, 72653–72658; c) M. Li, X. Xu, Y. Gong, Z. Wei, Z. Hou, H. Li, Y. Wang, *Green Chem.* **2014**, *16*, 4371–4377; d) P. Li, H. Liu, Y. Yu, C. Y. Cao, W. G. Song, *Chem. Asian J.* **2013**, *8*, 2459–2465; e) F. G. Cirujano, A. Leyva-Pérez, A. Corma, F. X. Llabrés i Xamena, *ChemCatChem* **2013**, *5*, 538–549; f) P. Liu, C. Li, E. J. M. Hensen, *Chem. Eur. J.* **2012**, *18*, 12122–12129.
- [4] a) M. Tamura, R. Kishi, Y. Nakagawa, K. Tomishige, *Nat. Comm.* **2015**, *6*, article no. 8580; b) Y. Liu, X. Xi, C. Ye, T. Gong, Z. Wang, Y. Cui, *Angew. Chem. Int. Ed.* **2014**, *126*, 13821–13825; c) Y. Zhang, B. Li, S. Ma, *Chem. Commun.* **2014**, *50*, 8507–8510; d) N. A. Brunelli, C. W. Jones, *J. Catal.* **2013**, *308*, 60–72; e) R. Srirambalaji, S. Hong, R. Natarajan, M. Yoon, R. Hota, Y. Kim, Y. Ho Ko, K. Kim, *Chem. Commun.* **2012**, *48*, 11650–11652; f) N. Raveendran Shiju, A. H. Alberts, S. Khalid, D. R. Brown, G. Rothenberg, *Angew. Chem. Int. Ed.* **2011**, *50*, 9615–9619; g) T. Takahashi, T. Watahiki, S. Kitazume, H. Yasuda, T. Sakakura, *Chem. Commun.* **2006**, *0*, 1664–1666.
- [5] a) M. Shakeri, C.-W. Tai, E. Göthelid, S. Oscarsson, J.-E. Bäckvall, *Chem. Eur. J.* **2011**, *17*, 13269–13273; b) E. V. Johnston, O. Verho, M. D. Kärkäs, M. Shakeri, C.-W. Tai, P. Palmgren, K. Eriksson, S. Oscarsson, J.-E. Bäckvall, *Chem. Eur. J.* **2012**, *18*, 12202–12206; c) Y. Han, S. S. Lee, J. Y. Ying, *Chem. Mater.* **2006**, *18*, 643–649.
- [6] A. K. Engström, E. V. Johnston, O. Verho, K. P. J. Gustafson, M. Shakeri, C.-W. Tai, J.-E. Bäckvall, *Angew. Chem. Int. Ed.* **2013**, *52*, 14006–14010.
- [7] a) S. Talekar, A. Joshi, G. Joshi, P. Kamat, R. Haripurkar, S. Kambale, *RSC Adv.* **2013**, *3*, 12485–12511; b) J. C. Lewis, *ACS Catal.* **2013**, *3*, 2954–2975.
- [8] J. Ge, J. Lei, R. N. Zare, *Nat. Nanotechnol.* **2012**, *7*, 428–432.
- [9] M. Felice, M. Marciello, M. del Puerto Morales, J. M. Palomo, *Chem. Commun.* **2013**, *49*, 6876–6878.
- [10] a) R. A. Sheldon, *Appl. Microbiol. Biotechnol.* **2011**, *92*, 467–477; b) R. A. Sheldon, *Org. Process. Res. Dev.* **2011**, *15*, 213–223.
- [11] T. Görbe, K. P. J. Gustafson, O. Verho, G. Kerrefors, H. Zheng, X. Zou, E. V. Johnston, J.-E. Bäckvall, *ACS Catal.* **2017**, *7* (3), 1601–1605.
- [12] General reviews on DKR: a) O. Verho, J.-E. Bäckvall, *J. Am. Chem. Soc.* **2015**, *137*, 3996–4009; b) R. Marcos, B. Martín-Matute, *Isr. J. Chem.* **2012**, *52*, 639–652. Reviews specified on DKR of amines: c) Y. Kim, J. Park, M.-J. Kim, *ChemCatChem* **2011**, *3*, 271–277; d) Y. Wang, H. Zhao, *Catalysts* **2016**, *6*, 194.
- [13] M. T. Reetz, K. Schimossek, *Chimia* **1996**, *50*, 668–669.
- [14] J. Paetzold, J.-E. Bäckvall, *J. Am. Chem. Soc.* **2005**, *127*, 17620–17621.
- [15] M. Shakeri, K. Engström, A. G. Sandström, J.-E. Bäckvall, *ChemCatChem* **2010**, *2*, 534–538.
- [16] A. N. Parvulescu, P. A. Jacobs, D. E. De Vos, *Appl. Catal. A* **2009**, *368*, 9–16.
- [17] G. Cheng, B. Xia, Q. Wu, X. Lin, *RSC Advances* **2013**, *3*, 9820–9828.
- [18] Q. Jin, G. Jia, Y. Zhang, C. Li, *Catal. Sci. Technol.* **2014**, *4*, 464–471.
- [19] G. Xu, X. Dai, S. Fu, J. Wu, L. Yang, *Tetrahedron Lett.* **2014**, *55*, 397–402.
- [20] M.-J. Kim, W.-H. Kim, K. Han, Y. K. Choi, *J. Org. Lett.* **2007**, *9*, 1157–1159.
- [21] K. Han, J. Park, M.-J. Kim, *J. Org. Chem.* **2008**, *73*, 4302–4304.
- [22] K. Han, Y. Kim, J. Park, M.-J. Kim, *Tetrahedron Lett.* **2010**, *51*, 5581–5584.
- [23] K. P. J. Gustafson, R. Lihammar, O. Verho, K. Engström, J.-E. Bäckvall, *J. Org. Chem.* **2014**, *79*, 3747–3751.
- [24] By-product arises from the hydrogenolysis of the C-N bond cleavage.
- [25] M. Cammenberg, K. Hult, S. Park, *ChemBioChem*, **2006**, *7*, 1745–1749.
- [26] Only two examples of such biohybrids as artificial metalloenzymes for DKR of amines were previously reported: see refs 6 and 9.